Optics & Laser Technology 78 (2016) 19–33

Contents lists available at ScienceDirect

Optics & Laser Technology

journal homepage: www.elsevier.com/locate/optlastec

Review

[INVITED] Tilted fiber grating mechanical and biochemical sensors ☆

Tuan Guo [a,*], Fu Liu [a], Bai-Ou Guan [a], Jacques Albert [b]

[a] Institute of Photonics Technology, Jinan University, Guangzhou 510632, China
[b] Department of Electronics, Carleton University, 1125 Colonel By Drive, Ottawa, Canada K1S 5B6

ARTICLE INFO

Article history:
Received 10 September 2015
Accepted 12 October 2015
Available online 22 October 2015

Keywords:
Photonics
Optical fiber
Grating
Bragg
Mechanical sensing
Biochemical sensing
Plasmonics

ABSTRACT

The tilted fiber Bragg grating (TFBG) is a new kind of fiber-optic sensor that possesses all the advantages of well-established Bragg grating technology in addition to being able to excite cladding modes resonantly. This device opens up a multitude of opportunities for single-point sensing in hard-to-reach spaces with very controllable cross-sensitivities, absolute and relative measurements of various parameters, and an extreme sensitivity to materials external to the fiber without requiring the fiber to be etched or tapered. Over the past five years, our research group has been developing multimodal fiber-optic sensors based on TFBG in various shapes and forms, always keeping the device itself simple to fabricate and compatible with low-cost manufacturing. This paper presents a brief review of the principle, fabrication, characterization, and implementation of TFBGs, followed by our progress in TFBG sensors for mechanical and biochemical applications, including one-dimensional TFBG vibroscopes, accelerometers and micro-displacement sensors; two-dimensional TFBG vector vibroscopes and vector rotation sensors; reflective TFBG refractometers with in-fiber and fiber-to-fiber configurations; polarimetric and plasmonic TFBG biochemical sensors for *in-situ* detection of cell, protein and glucose.

Contents

☆Invited Article by the Associate editor: Christophe Caucheteur.

* Corresponding author.
E-mail address: tuanguo@jnu.edu.cn (T. Guo).

http://dx.doi.org/10.1016/j.optlastec.2015.10.007

1. Introduction

The field of optical fiber technology has experienced an interesting return towards its sources over the past few years. Because of the need for ever increasing communication capacity, transmission systems based on multimode optical fibers are being developed for mode multiplexing applications [1–4]. The same is true for optical fiber sensors where there is a growing interest in using the simultaneous but differential response of optical fiber modes to perturbations as a means of increasing the sensitivity, capacity, or limits of detection (LOD) in sensing systems [5,6]. In order to access these improved functionalities however, some form of mode control is required. While complex mode launching instrumentation based on free space optics can be used in telecommunications, such complexity is prohibitively expensive in sensing. In optical fiber sensors, mode control is most easily achieved from a fiber with single mode core by using a grating to couple from this well-defined starting point to higher order modes at specific wavelengths determined by the phase matching condition of the grating [7–15]. Polarization control is also useful and often necessary, especially in sensing applications involving surface plasmon resonance (SPR) or other "plasmonic" effects [16–19]. The first widespread grating-assisted multimodal optical fiber sensors relied on long period gratings (LPGs) that couple core guided light to forward propagating cladding modes of the same fiber. It is with LPGs that the wide range of sensing modalities that are possible with cladding modes was discovered [12]. Unlike the core mode, cladding modes properties are sensitive to bending and to the surrounding refractive index for instance. Furthermore these sensitivities vary widely from mode to mode, as mode field shape, effective index and polarization depend strongly on mode order and launching conditions. The final great advantage is that conventional single mode fibers (of any kind, including low cost telecommunication fibers and plastic optical fibers) inherently guide hundreds of cladding modes without further modification because of the large size of the cladding diameter relative to wavelength.

LPGs for sensing have limitations however. In "normal" LPGs with grating induced index change that is azimuthally symmetric in the fiber cross section, only modes with the same azimuthal symmetry as the incoming core mode can be excited and polarization control is difficult if not impossible. In polarization selective applications, it means that half the light is "wasted", i.e. not participating in the sensing mechanism and thus contributing to a high background signal (and reduced signal to noise ratio). This can be improved upon however by using the "excessively tilted" grating structures developed by Zhou and Zhang et al. at Aston University in the UK [20–22], where LPGs with tilted grating planes are used, thereby breaking the azimuthal symmetry and allowing the excitation of polarization distinct cladding modes in many important applications, including in-fiber polarizers [23–25], lasers [26–28], sensors [29–31] and spectral interrogators [32–38]. The main drawback of LPGs however comes from their perceived advantage: the grating phase match condition between an incident core mode and the cladding modes depends on the DIFFERENCE between the effective indices of the two modes being coupled. Because of the relative dispersion of the two modes, the resonance wavelength of these couplings can be made extremely sensitive to select perturbations, and this is considered very good for sensing applications. However, by the same principle such cladding mode resonances are sensitive to everything and it is nearly impossible to eliminate cross-talk between the desired measurand and other effects, most notably temperature or small bends.

The present paper describes a structure that is apparently similar to a LPG but differs in many important aspects. A tilted fiber Bragg grating (TFBG) has a grating period similar to that of a regular fiber Bragg grating (FBG), i.e. roughly one third of the wavelength (in glass fibers) but grating planes that are weakly tilted relative to the fiber axis. Similar to LPGs, this tilt enables strong coupling between the core mode and select cladding modes but the phase matching condition is different, as the resonance wavelength depends on the SUM of the effective indices (the corresponding theory was developed by Erdogan et al. at Rochester University in the US [39–41] and in many other follow up papers [42–53]). This makes resonance positions much less sensitive to perturbations but much more controllable in real applications [54–60]. Furthermore, the phase matching condition also implies that the linewidth of resonances is orders of magnitude smaller than LPGs and that the spacing between individual resonances is much smaller, meaning that hundreds of resonances can be measured simultaneously and compared using a spectral range of less than 100 nm. In the remainder of this paper, the fabrication and properties of TFBGs and their transmission/reflection spectra will be described, followed by a review of their sensing applications, with special emphasis on mechanical sensing for structural health monitoring and biochemical sensing for *in-situ* medical detections.

2. TFBG fabrication and sensing principle

2.1. Fabrication

TFBGs are fabricated using the same tools and techniques as standard FBGs, i. e. from a permanent refractive index change induced in doped glasses by an interference pattern between two intense ultraviolet laser beams [61], or a point by point approach [62]. In general however, the phase mask technique [63–66] is preferred for mass produced FBGs. In this case, the interference pattern is generated by a diffractive phase mask located in close proximity to the fiber. The period of the grating is fixed by the phase mask and because of the proximity of the fiber, low coherence ultraviolet sources can be used, such as high energy pulsed excimer lasers. With a phase mask, tilting can be done in two ways: rotating the phase mask and fiber consistently around an axis perpendicular to the laser beam (phase mask and fiber are kept parallel), or keeping the fiber and phase mask perpendicular to the incident writing beam but rotating the phase mask around the axis of the writing beam. We have found by experience that rotating the fiber phase mask assembly by the former technique (inset of Fig. 1) provides the best spectral responses for strong TFBGs with tilt angles between 4° and 30°. We use an excimer laser operating at 193 nm wavelength to make TFBGs in standard single mode fibers that have been hydrogen-loaded to enhance their photosensitive response.

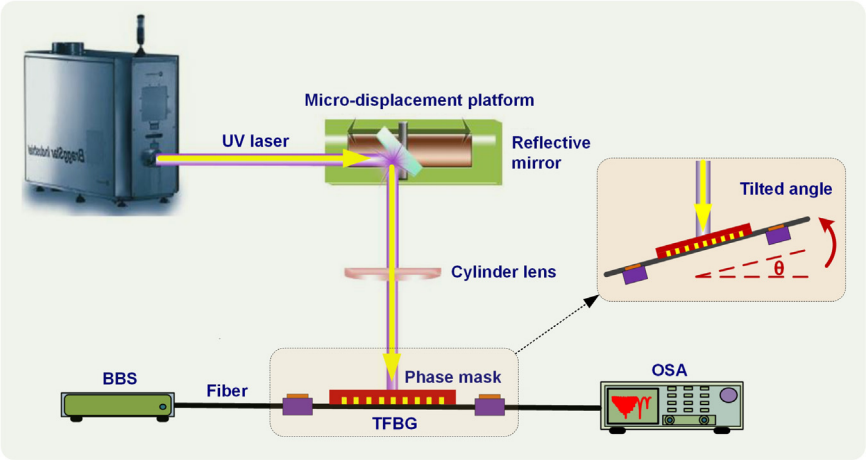

Fig. 1. TFBG inscription system based on phase mask assembly rotation technique (inset).

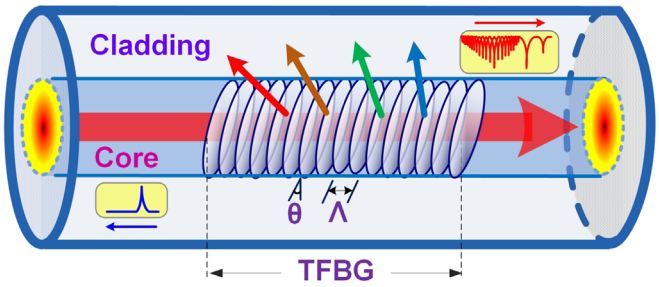

Fig. 2. Sketch of the configuration of the TFBG.

2.2. Configuration and spectral character

Fig. 2 presents the configuration of the TFBG. Incoming core guided light interacts with a permanent refractive index grating that has been inscribed in the fiber by intense ultraviolet light irradiation through a diffractive phase mask. A tilt in the orientation of the grating planes favors the coupling of light to modes guided by the cladding instead of the core. Since the cladding diameter is very large ($>100\,\mu m$, almost 100 times the wavelength) a large number of modes can be excited, each at a specific wavelength, resulting in a fine comb of resonances (hundreds of) in the transmission spectrum of the grating (Fig. 3). The tilt of the grating is an important parameter that can be used to choose which set of cladding modes is going to be excited (Fig. 3),

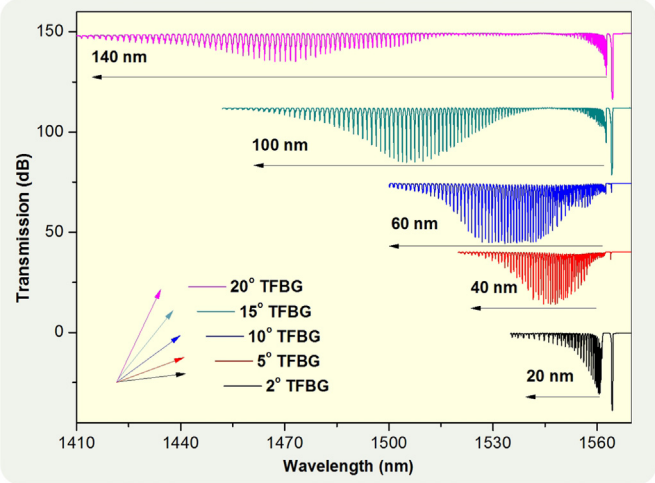

Fig. 3. Measured TFBG transmission spectra as a function of tilt angle.

over the range from tens of nanometers to more than one hundred nanometers. As a result, it makes it possible to adjust the operating range of the sensor in order to optimize the response for different kinds of perturbations (Fig. 4).

2.3. Sensing principle

2.3.1. Core mode

The core mode of a TFBG is identified by the resonance with the longest wavelength and it is the most confined mode. This resonance presents the same temperature (10 pm/°C) and axial strain (1 pm/με) sensing characteristics as that of standard FBGs, and it is inherently insensitive to events outside the cladding. Because all the core and cladding mode resonances have the same temperature dependence and hence shift together with temperature, the temperature cross sensitivity of most other sensing modalities can be removed simply by measuring relative wavelength shifts (relative to the core mode resonance for instance) instead of absolute wavelengths [67].

2.3.2. Ghost modes

The ghost modes of TFBG are a group of strongly guided cladding modes which interact much with core–cladding interface but little with the outside fiber boundary [68]. It is because their resonances are adjacent to the core mode (approximately 2 nm away on the shorter wavelength side) and most often form a single resonance that is spectrally similar (in amplitude and width) with that of core mode, that they are named “ghost” modes.

To gain a better understanding of the characteristics of the ghost modes we used numerical mode simulation (OptiGrating) to analyze the composition of the ghost resonance and the transverse electric field amplitude distributions of its constituent modes [69]. We model the modes of a TFBG with a 4° tilt angle and Bragg resonance centered at 1550 nm. Among low order LP_{nm} modes ($n=0$–3) we found that the first order odd LP_{1m} modes with $m=1$–4 contribute most to the ghost resonance. Fig. 5 shows the amplitude distributions and transmission spectra of the basic low order cladding LP_{nm} modes and the first-order odd LP_{1m} modes which contribute most to the ghost resonance (the red curves of the inset in Fig. 5). Because these first-order odd modes are adjacent to the core–cladding interface with an asymmetrical distribution, any slight fiber bending may induce a change in their transverse electric field amplitude distributions. With help from a discontinuity in the core (like off-set splicing, taper or core-diameter mismatching [13]), such ghost modes can be recaptured back to the fiber core with high efficiency. And the recoupling

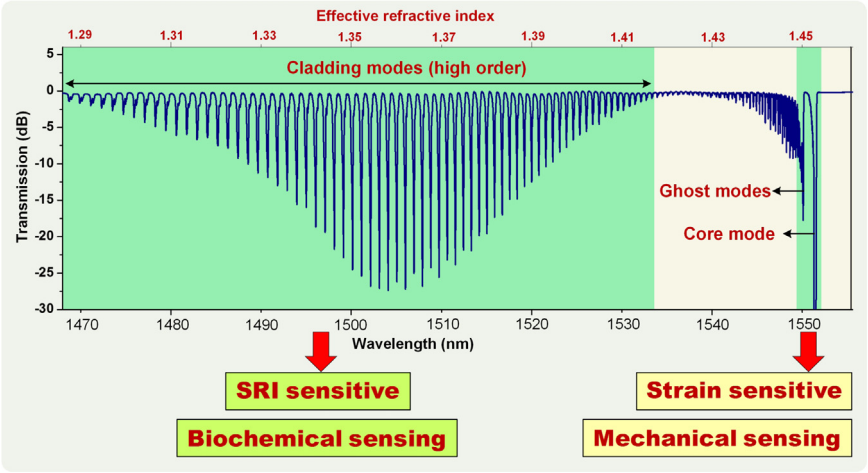

Fig. 4. Mechanical and biochemical sensing based on TFBG cladding modes with wide spectral coverage.

efficiency at the junction is strongly modulated, providing very highly sensitive fiber-optic mechanical sensors like bending, rotation, lateral pressure or vibration sensors (more details are discussed in Section 3). Although the combined spectrum of the resonances making up the ghost resonance is complicated and irregular, it does not matter as we can measure the total power in the spectral band covering the whole resonance, not the detailed spectral shape.

2.3.3. *High order cladding modes*

Further resonances at decreasing wavelengths correspond to cladding guided modes with increasing amounts of evanescent fields extending outside the cladding boundary (typically over a thickness of the order of 2 μm above the cladding surface) [70,71]. When the immediate environment of the TFBG changes within the region sampled by the mode evanescent fields, the resonance positions of the corresponding cladding modes change accordingly (Fig. 6a). The largest resonance shift occurs when the evanescent field of the modes overlaps maximally with the perturbation, usually for the least guided resonances, i.e. at the shortest wavelengths. However, at further decreasing wavelengths there comes a point at which the grating couples light to modes that are no longer guided by the cladding. These leaky modes have resonance positions that do not shift in wavelength in response to surrounding refractive index (SRI) changes, but only in amplitude. The boundary between guided and leaky modes is called the “cut-off

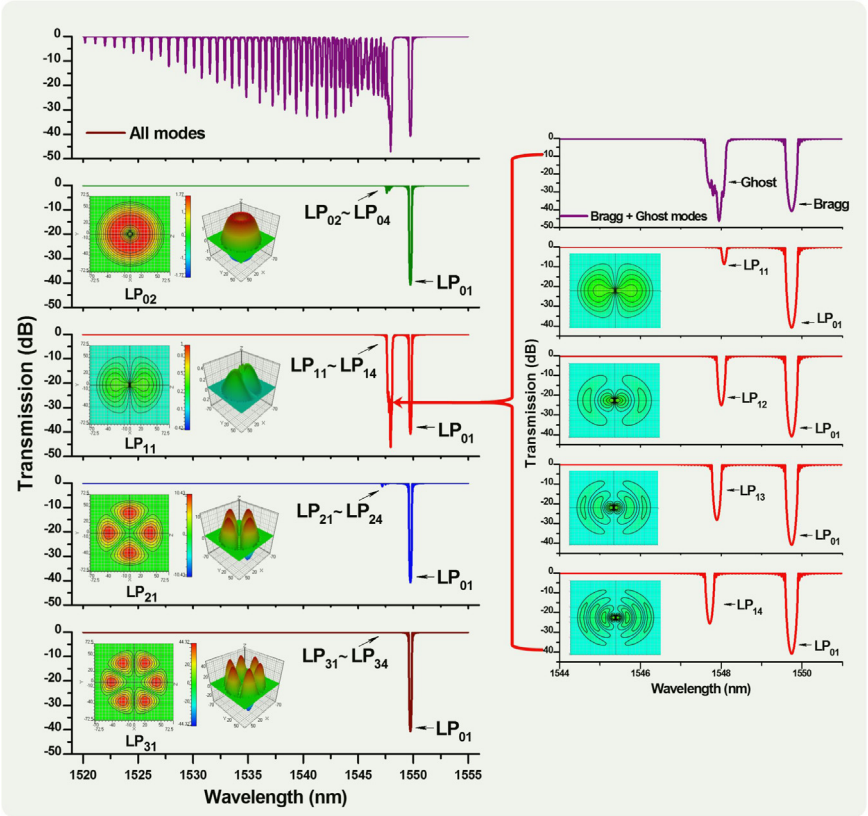

Fig. 5. Numerical analysis of the composition of the ghost modes in a 4° TFBG: the amplitude distributions and transmission spectra of the basic low order cladding LP_{nm} modes and the first-order odd LP_{1m} modes (inset). (For interpretation of the references to color in this figure, the reader is referred to the web version of this article.)

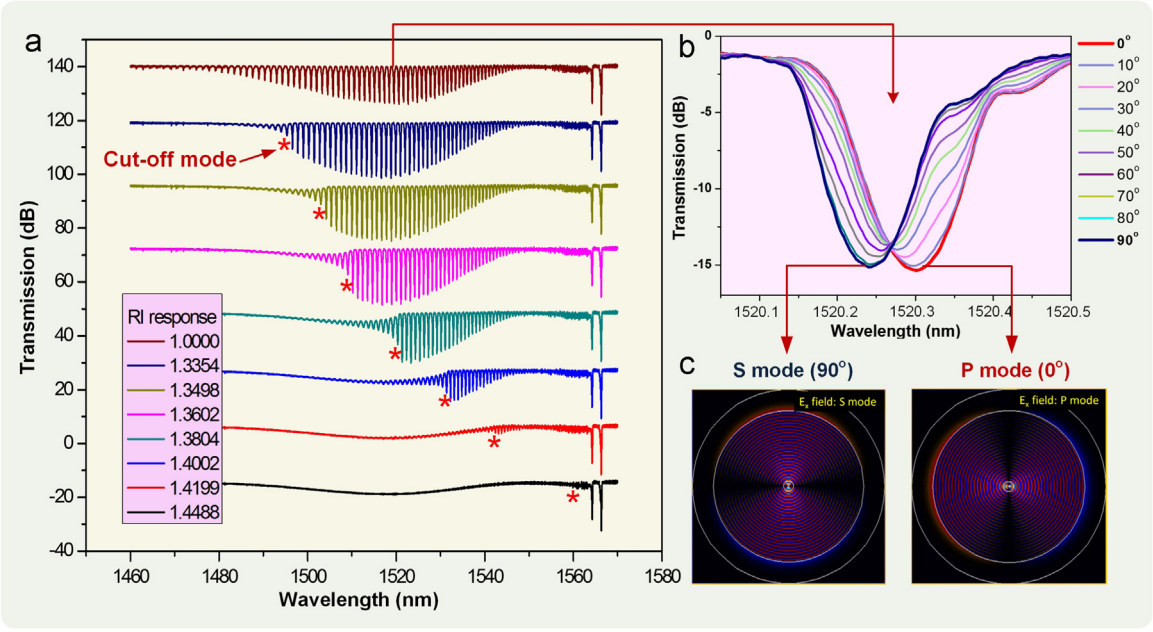

Fig. 6. Measured spectral transmission characteristics of a 12° TFBG: (a) versus surrounding RI and (b) versus different orientations of the input light polarization, (c) the simulated horizontal component of the transverse electric field of representative S and P modes near "cut-off". Note: the "cut-off" mode is marked by red asterisk "*". (For interpretation of the references to color in this figure legend, the reader is referred to the web version of this article.)

point" (evidenced by reduced amplitude of the cladding mode resonance, as indicated by the red stars in Fig. 6a) and the last guided mode before this point has the maximum extent of evanescent field penetration in the external medium (and hence the largest sensitivity). The operating point (i.e. the range of wavelengths where modes have maximum sensitivity, near the "cut-off point" for instance) determines the choice of tilt angle: increasing the tilt angle shifts the maximum of the resonance amplitudes towards lower wavelengths.

Moreover, a further mode selection mechanism (i.e. polarization) can be used to refine the sensing capabilities of the TFBG [72–74]. By launching linearly polarized light in the core (polarization rotated from 0° to 90° relative to the tilt plane), cladding-guided resonances with strong polarization dependence have been obtained. Fig. 6b presents two very different families of cladding modes that can be selected: modes with radially polarized evanescent fields (hereafter named P-modes, as they are excited by core guided light that is P-polarized relative to the tilt plane), and modes with azimuthally polarized evanescent fields (excited by S-polarized core mode). Fig. 6c shows the horizontal component of the electric field for representative S- and P-modes. Since S- and P-modes have different reflection characteristics at the boundary: S-modes have their electric field parallel to the cladding boundary and P-modes are perpendicular. A comparison of the relative changes observed in a pair of S- and P-modes provides a self-referenced tool to measure even smaller changes at the cladding surface than un-polarized TFBGs [75]. This technique will be introduced in Section 4.

2.3.4. *Surface plasmon resonances*

So called "Surface Plasmon Resonance", or SPR, sensors are devices that can measure the effective index of plasmons and their changes in response to modifications in a thin layer close to a metal surface [76]. The plasmons that are actually used for sensing

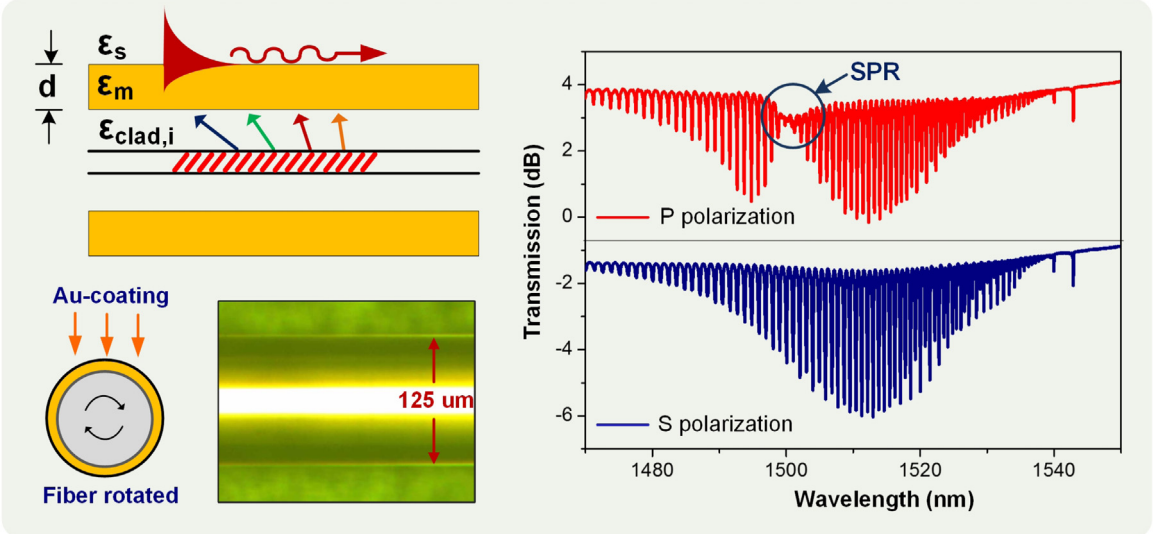

Fig. 7. Schematic diagram and photograph of gold-coated plasmonic TFBG and its transmission spectra versus P and S input polarizations.

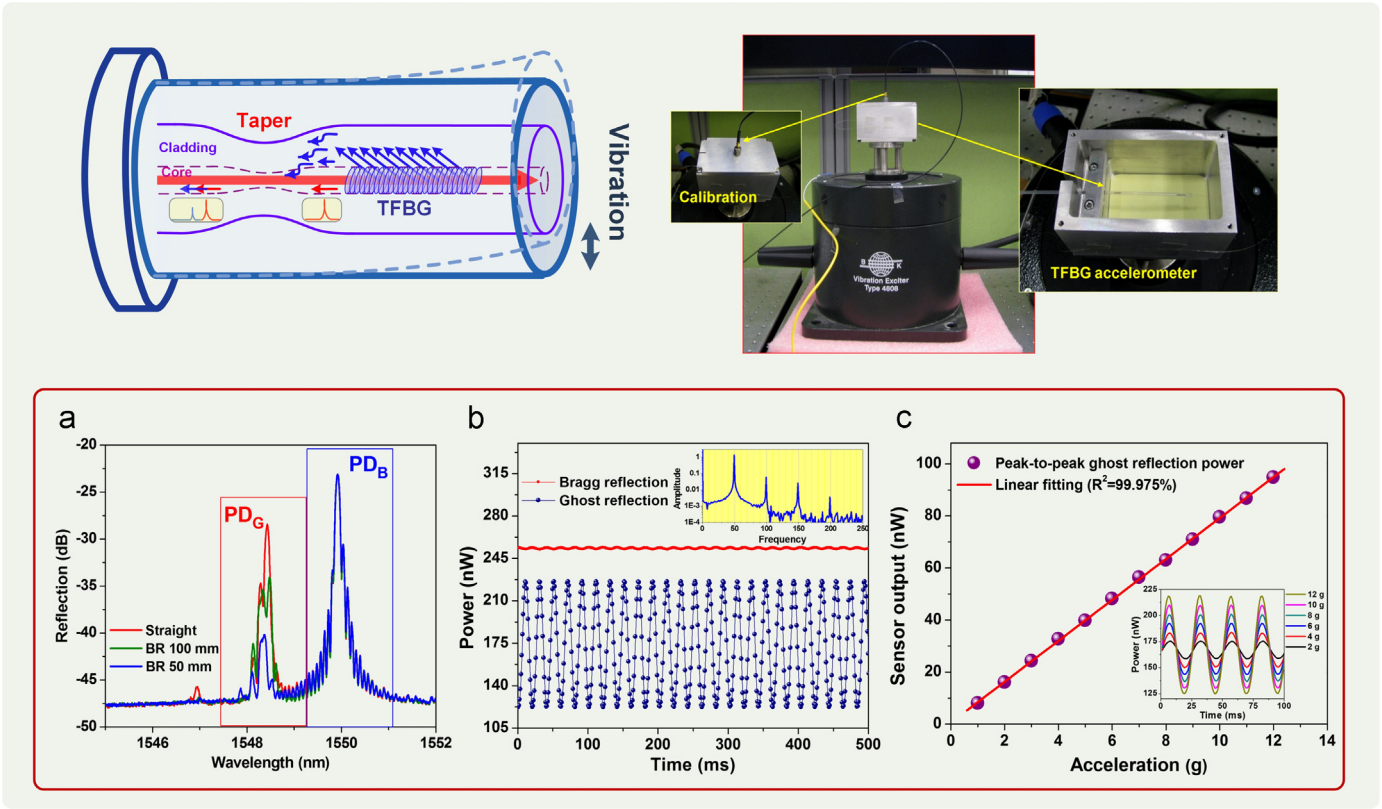

Fig. 8. One-dimensional accelerometer (TFBG with an abrupt biconical taper) [69].

are hybrid waves that have intense field localization at the outer surface of a metal film deposited on a solid dielectric support (Fig. 7). When the SRI of the outer medium is smaller than that of the solid support, a propagating wave incident from the support side can be totally internally reflected at the support metal boundary but phase-matched to a quasi-plasmon excitation at the outer boundary of the metal. In order for this coupling to occur, the incident wave must be polarized in the plane of incidence (i. e. TM- or P-polarized) and the metal layer must be thin enough to let some light tunnel across. It is the tunneling wave that excites the quasi-plasmon and when this coupling occurs the reflected wave loses power and the corresponding cladding mode resonance loses amplitude (Fig. 7).

In order to effectively excite and accurately measure plasmon resonances and hence to achieve this optimum sensitivity, SPR based TFBG sensors have been developed and well studied [77–83]. There are two unique features of TFBGs: the strong polarization selectivity (comes from the breaking of the cylindrical symmetry of non-polarization-maintaining fibers) and the high-density comb of narrowband spectral resonances. This makes it possible to excite SPR and to measure their spectral location with quality factors between 10^3 and 10^4. Therefore, SPR based TFBG sensors open up a multitude of opportunities for single-point biochemical sensing in hard-to-reach spaces, and offer an extremely improved LOD level to molecular interactions together with very controllable cross-sensitivities.

3. TFBG mechanical sensors

Structural health monitoring is a critical issue in various engineering applications, especially for civil engineering, energy and the aerospace industry. Mechanical sensors play an important role for understanding and evaluating the health status of such structures. Over the last ten years, multimodal and multifunctional fiber-optic mechanical sensors based on TFBG have been developing, including bending sensors [84–88], inclinometer [89,90], lateral force sensors [91,92], displacement sensors [93], twist sensors [94–97], vibroscopes [68,98–100], accelerometers [69], and microwave [101,102] and interrogation components [103–106]. The devices discussed herein benefit from the following desirable features: (i) linear response (less than 1% deviation from linearity over the measurement range), (ii) cost-effective interrogation (measure of power rather than wavelength), (iii) self-calibration (power fluctuations from the light source and transmission line can be canceled out by referring to a spectrally separated Bragg resonance which is immune to vibration and slight bending), (iv) elimination of temperature cross-sensitivity (the power response of the detected cladding resonances are insensitive to temperature), (v) compact size (10∼20 mm in length and diameter less than 2 mm); (vi) suitability for embedding in engineered structures (the sensors work in reflection). These TFBG mechanical sensors are aimed at applications where optical sensors are preferred over electrical ones, for example, long term structural health monitoring of relatively large structures where a number of sensors need to be embedded and connected, or for applications where light weight and immunity to electromagnetic interference is critical.

3.1. One-dimensional TFBG mechanical sensors

As discussed in Section 2, ghost modes are low order cladding modes and they are very sensitive to fiber bending (both static and dynamic). However, they do not show up in reflection because they cannot propagate for a long distance along the fiber cladding owing to the absorption of the high-index jacket material. However, when the fiber is kept straight and the cladding is not covered by absorbing material, such modes can propagate for several

centimeters without much loss. Therefore, the key point is that if we can induce a "bridge" located a short distance upstream of the TFBG so that the ghost modes can be effectively recaptured back to the fiber core, then they can propagate back to the interrogation system with low loss. Over the last few years, various "bridge" configurations have been reported, such as using a offset splicing [68], an abrupt biconical fused taper [69,89] to recouple light from the cladding modes to the core for vibration, acceleration and inclination measurement, and using a core-diameter mismatched fiber section as cladding mode coupler [86,107] for bending sensors and refractometers.

3.1.1. Accelerometer

Fig. 8 presents a fiber-optic accelerometer comprising a TFBG and an abrupt biconical taper, all encapsulated in a plastic tube using a rigid ultraviolet-cured acrylate epoxy [69]. The electric-arc-heating induced taper is located a short distance upstream from the TFBG and functions as a bridge to recouple the TFBG-excited lower-order cladding modes back into the fiber core. This recoupling is extremely sensitive to microbending (Fig. 8a, PD_G). We avoid complex wavelength interrogation by simply monitoring the power change in reflection, which we show to be proportional to acceleration (Fig. 8c). In addition, the Bragg resonance is virtually unaffected by fiber bending (Fig. 8a, PD_B) and can be used as a power reference to cancel out any light source fluctuations. The proposed accelerometer provides a constant linear response (nonlinearity $< 1\%$) over an acceleration range from 0.5 to 12.5 g, a flat amplitude sensitivity over a vibration frequency range from DC to 250 Hz and a adjustable resonance frequency by simply varying the sensor length. The composite structure is very stiff to ensure a good transfer of the vibrations from the tube to the TFBG and provides long term protection, even in harsh environments.

3.1.2. Micro-displacement sensor

Fig. 9 presents a novel method for micro-displacement measurement based on a non-uniform tilt modulation of a weak TFBG [93]. A metal bending cantilever beam is used to provide a displacement-induced Gaussian-strain-gradient along the sensing TFBG (Fig. 9, precisely pasting the TFBG at the center Gaussian-strain gradient region is essential to maximize the sensor quality). The internal tilt angles of the grating fringes are modulated non-uniformly via the displacement-induced Gaussian-strain-gradient and a dramatically weakened core-to-cladding mode coupling is achieved (Fig. 9a) due to the phase mismatch between different grating pitches. Compared to the same beam with a straight FBG but Bragg reflection monitoring, the power response of the ghost resonance in transmission shows an extremely improved sensitivity (12 times higher) to the displacement change (Fig. 9b). The proposed sensor provides a constant linear response over a displacement range of several millimeters (dependent on the size of supporting beam) and it is immune to a spatially uniform temperature variation (less than 4% full scale for a temperature variation from 0 °C to 90 °C).

3.2. Two-dimensional TFBG vector mechanical sensors

Orientation information is essential in many branches of mechanical measurement. For example, a precise identification of the orientation of a vibration is a key point to find the position an unknown or dynamically changing vibration source, in seismic detection for instance. Traditional methods normally use several separate sensors oriented orthogonally to measure two dimensional or three dimensional strain fields and waves. This results in sensors suffering from a complex configuration and unavoidable cross-talk between vibration or bending directions. The question is how to use a single detector to achieve an orientation-recognized mechanical measurement, i.e. a vector measurement. The polarization dependency of high-order modes in TFBGs provides a potential way for orientation-recognized sensing. Wavelength and polarization control allows the users to select only EH modes (oriented radially at the cladding boundary) or HE modes (oriented tangentially at the cladding boundary), as well as modes with well defined azimuthal power distributions across large portions of the spectrum. Therefore, any vector sensing modality that depends strongly on the polarization state and mode power distribution of the light near the cladding boundary can be

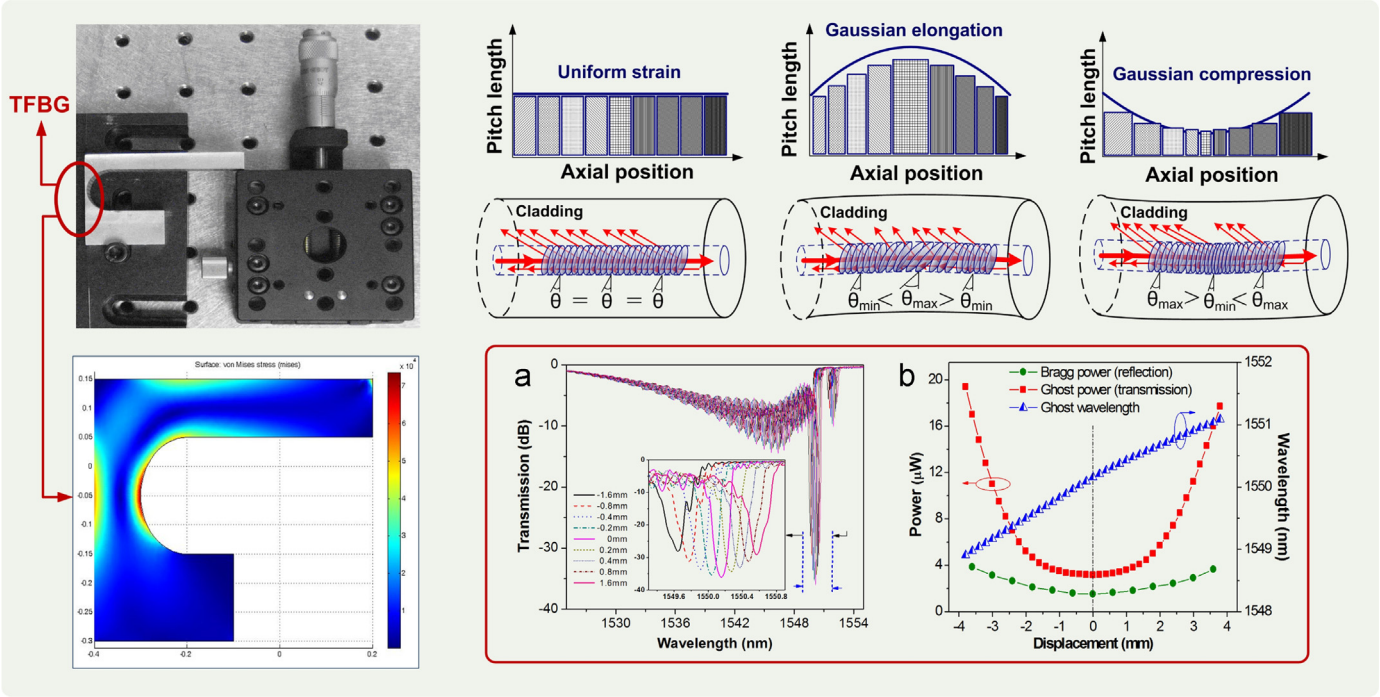

Fig. 9. One-dimensional micro-displacement sensor (TFBG with a non-uniform tilt modulation) [93].

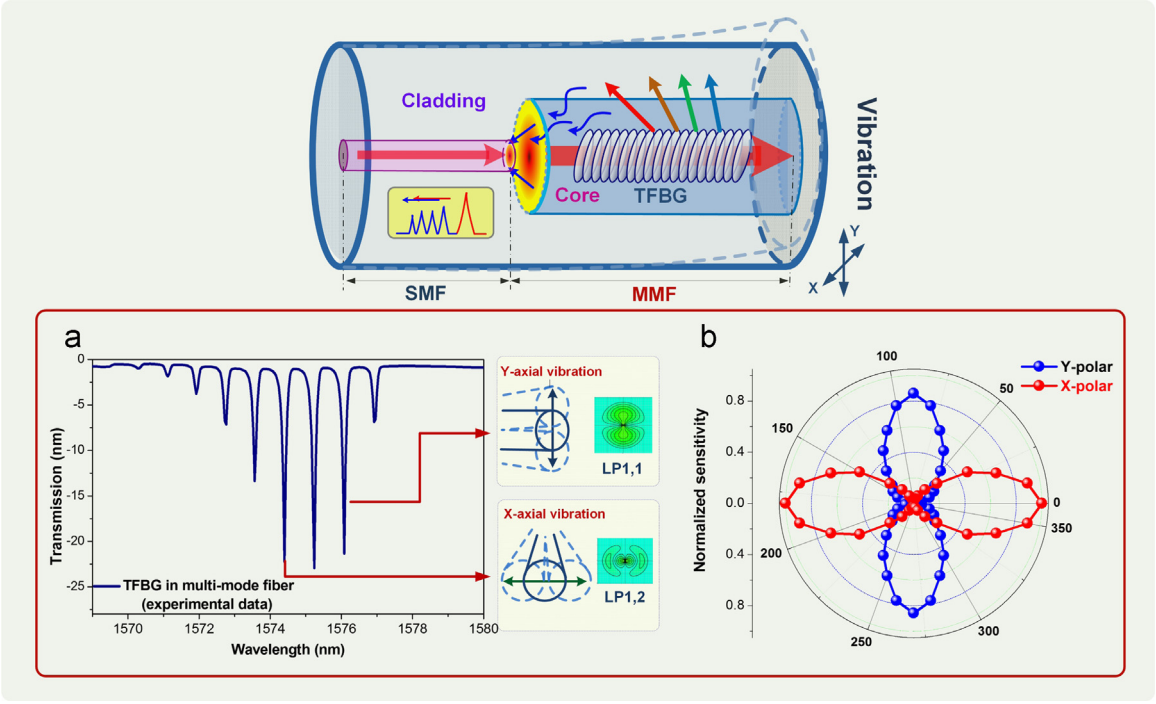

Fig. 10. Two-dimensional vibroscope (MMF-TFBG using orthogonal-polarimetric detection) [100].

measured very effectively with TFBGs [88,89].

How to transfer such strong polarization dependence from high-order cladding modes to low-order modes (strongly guided and influenced by core perturbations, but little by contact with the cladding boundary)? A TFBG inscribed in multi-mode fiber (MMF) provides a potential solution due to the physically "enlarged" fiber core. We now demonstrate two our proposed sensors for vector mechanical measurement by using such polarization-controlled core modes in MMF-TFBGs [95].

3.2.1. *Vector vibroscope*

Fig. 10 presents the two-dimensional vector vibration sensor based on polarization-controlled cladding-to-core recoupling [100]. A compact structure in which a short section of MMF stub containing a weak TFBG is spliced to another single-mode fiber without any lateral offset. Multiple core modes of the MMF are coupled at the junction and appear as well defined resonances (at different wavelength) in reflection from the TFBG. The LP_{11} and LP_{12} resonances are with orthogonal orientations and exhibit a strong polarization and bending dependence (Fig. 10a). Both the orientation (0–360°) and the amplitude of the vibrations can be

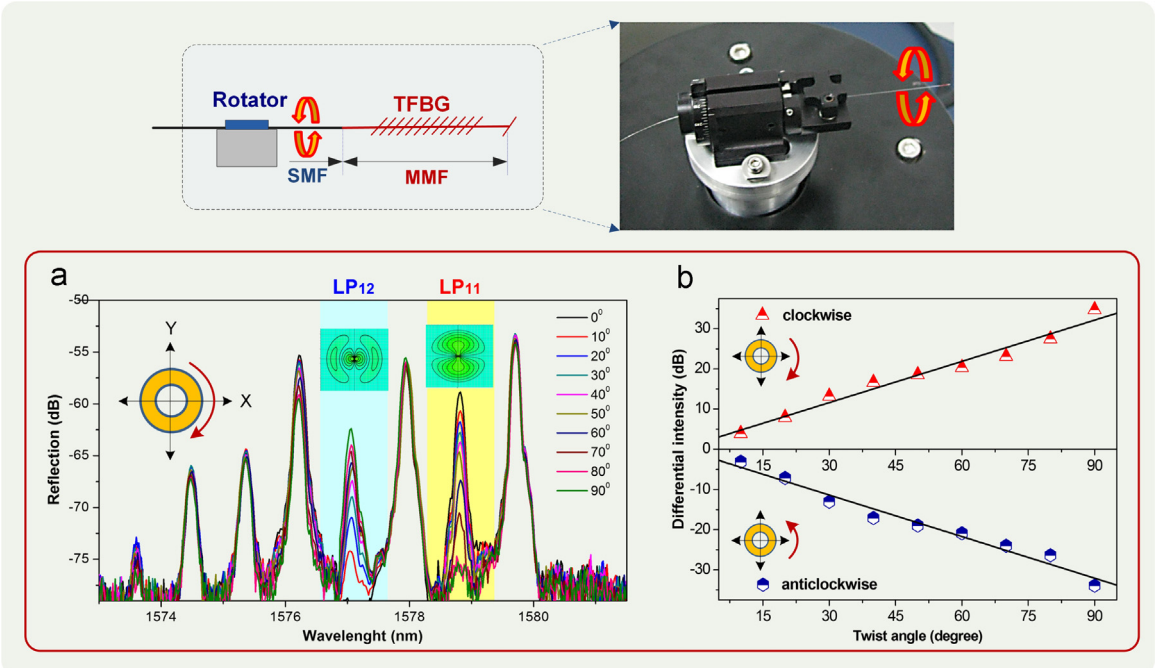

Fig. 11. Two-dimensional vector rotation sensor (MMF-TFBG using orthogonal-polarimetric detection) [95].

determined unambiguously via dual-path power detection of the orthogonal-polarimetric lowest order LP_{1n} modes (Fig. 10b). Meanwhile, the unwanted power fluctuations and temperature perturbations can be referenced out by monitoring the fundamental LP_{01} mode resonance.

3.2.2. Vector rotation sensor

Fig. 11 presents orientation-recognized rotation sensor using a polarimetric MMF-TFBG [95]. The larger diameter fiber core (62.5 μm) and graded index core/cladding profile enable the tilted gratings to excite multiple high order core modes with significantly different polarization dependence and to form a well-defined "comb" of spectrally separated resonances at different wavelengths (Fig. 11a). Orientation-recognized rotation measurements (−90° to 90°) have been achieved with sensitivity of 0.075 dB/° by using intensity monitoring of two orthogonally polarized odd core-modes, i.e. LP_{11} and LP_{12} (Fig. 11b). The proposed sensor is compact, works in reflection, is insensitive to temperature (intensity detection instead of wavelength monitoring) and is immune to unwanted intensity fluctuations (differential intensity measurement).

4. TFBG biochemical sensors

The use of optical fiber devices as biochemical sensors presents many well-known desirable features (size, cost, feasibility) for label-free methods as they contribute to the overall reduction in costs and ease of use factors [108,109]. Fiber optic sensors can be easily inserted into the media to be sensed (instead of having to bring samples inside an instrument) either as a hand held probe or as a set of remotely operated devices along a fiber optic cable (in environmental monitoring applications for instance).

Most kinds of optical fiber refractometers work through the perturbation of modal effective indices induced by changes in the SRI. One of the issues associated with such devices is that in order for the perturbation to be large, i.e. for the refractometer to be sensitive, the modal field considered must overlap strongly with the region where SRI changes are to be measured. In practice, it means that the highest sensitivity is achieved when the modes involved in the measurement are close to their wavelength cut-off point and hence extend far outside of their waveguiding layers. Because of this, most types of glass fiber refractometers reported so far achieve their highest sensitivities for SRI values larger than 1.4, i.e. for indices that are approaching that of the glass guiding media. However, there are many important applications for refractometers that operate in water or water-based solutions (including most biological and many environmental applications) where the SRI values are significantly lower, near 1.33 at optical wavelengths.

Moreover, it should be noted that for biochemical sensing fields, it is usually necessary to improve the LOD levels to at least 10^{-5} RIU, by increasing the wavelength shift sensitivity while keeping noise level down and spectral features narrow [110]. Fortunately, it has been recently demonstrated that the addition of a nanometric-scale gold or silver coating overlay on the optical fiber outer surface considerably enhances the refractometric sensitivity through the generation of surface plasmon resonance. The increased sensitivity achieved with plasmon waves arises because of the large localization of electromagnetic energy in the layer immediately adjacent to the metal surface. Any perturbation in that layer, such as the bonding of analytes on receptor molecules modifies the local RI of the dielectric and the plasmon phase velocity.

In recently years, a large number of multimodal and multifunctional fiber-optic refractometers and biochemical sensors based on TFBG and SPR have been developed, such techniques including: a combination of precise polarization control [72–75]; hybrid grating configurations [111–114]; coating the TFBG with functionalized materials [115–123]; enabling the multiplexing of TFBGs [124,125]; interrogating the TFBG in reflection [126–128]; simplifying the detection by using power instead of wavelength shifts [129–133]; and functionalizing the sensor for surface plasmon resonance excitations by coating the grating with uniform nanoscale metal films and thus without a requirement to etch or taper the fibers [77–80,134–143].

4.1. Reflective TFBG refractometers

The refractometers discussed herein benefit from the following desirable features: (i) shift the highest sensitivity from high SRI value (glass guiding media around 1.45) to low SRI value (water or water-based solutions close to 1.33), (ii) measure power rather than wavelength for cost-effective interrogation, (iii) the self-referenced core mode detection (independent of SRI) provides a normalization signal that is proportional to the light source power and therefore canceled out possible power fluctuations, (iv) the sensor works in reflection and the length of the entire sensor "head" can be very small (as little as 10–20 mm) so that the sensing probe can be easily inserted into the media to be sensed.

4.1.1. In-fiber reflective refractometer

Fig. 12 shows a novel in-fiber structure for power-referenced refractometry with the capability to measure SRI as low as 1.33 [127]. The sensor is based on strong cladding to core recoupling. A short optical fiber stub containing a weakly tilted Bragg grating is spliced to another fiber with a large lateral offset. The reflection from this structure occurs in two well-defined wavelength bands, the Bragg reflected core mode and the cladding modes (Fig. 12a). The cladding modes reflect different amounts of power as the SRI changes, while the core-mode reflection from the same weakly tilted FBG remains unaffected by the SRI (Fig. 12b). The measured sensitivity is up to 1100 nW/RIU for low SRI close to 1.33, and the noise power of the sensing system is less than 10 nW. Meanwhile, the power reflected in the core mode band can be used as a reliable reference to cancel out any possible power fluctuations.

4.1.2. Fiber-to-fiber reflective refractometer

Fig. 13 presents a recently developed tip-reflective and power-referenced refractometer based on strong fiber-to-fiber optical coupling for a large range of SRI (from 1.33 to 1.45) [133]. A short D-shaped fiber stub is placed in parallel and close contact to another standard circular fiber containing a weak TFBG. The TFBG couples the light from the circular fiber's core into its cladding where it remains guided. Apart from the direct light coupling over the contact interface, the evanescent field from the guided cladding modes penetrates the surroundings and reaches the D-fiber core by tunneling across the medium into which the fiber pair is located (Fig. 13a). The amount of tunneling depends strongly on the SRI so that the total amount of light collected by the D-fiber provides a measure of the SRI (Fig. 13b). Sensitivities ranging from 1000 to 13,000 nW/RIU have been obtained and the result is independent of temperature (within ± 10 nW of uncertainty). The measurement can be temperature-referenced through measurement of the TFBG spectrum if needed.

4.2. Polarimetric and plasmonic TFBG biosensors

The biochemical sensors discussed herein are aimed at biomedical applications where rapid, low consumption and highly sensitive detection of analytes at low concentrations are preferred. State-of-the-art nanometric-coating together with precise

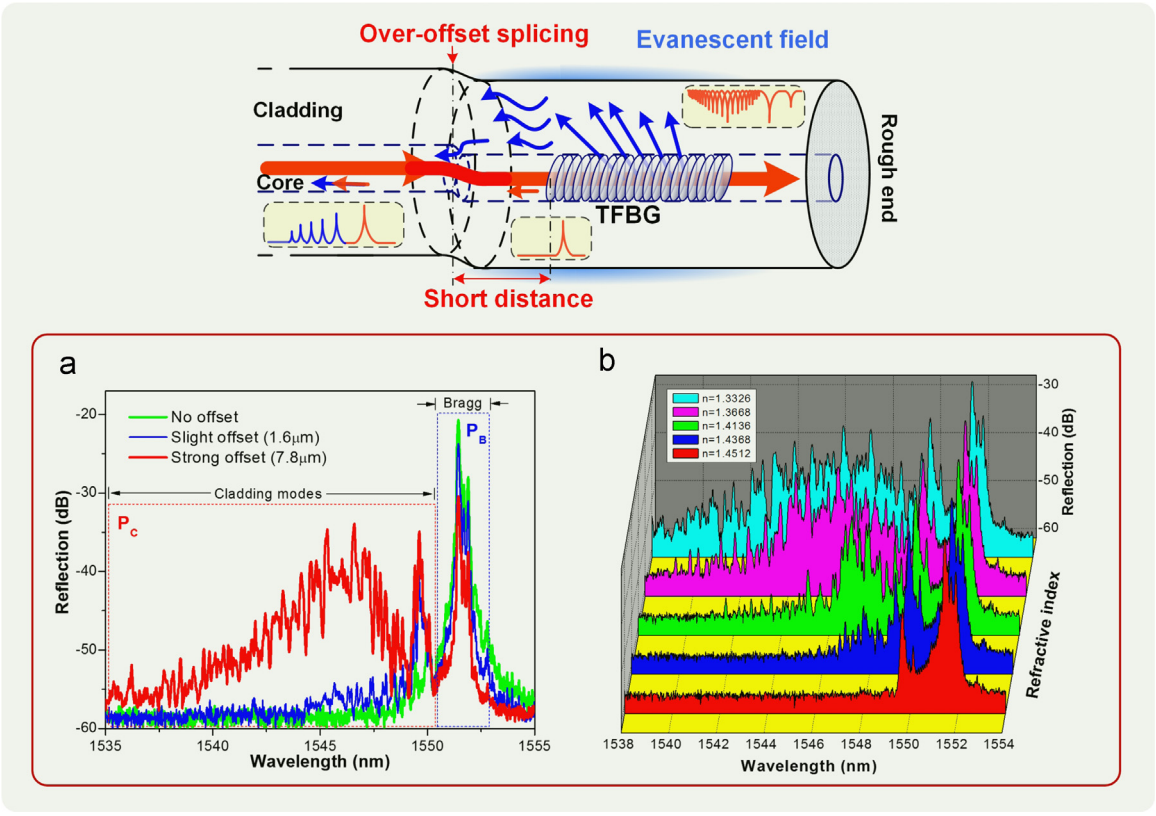

Fig. 12. In-fiber reflective refractometer (TFBG with an over offset splicing) [127].

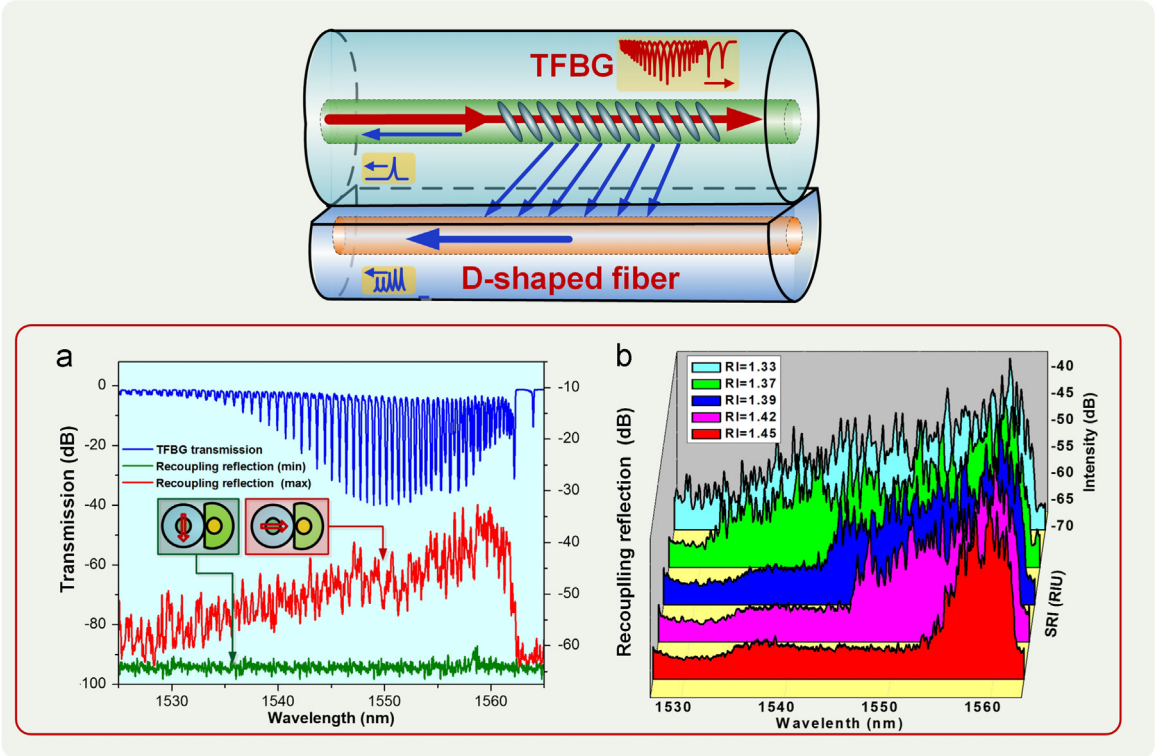

Fig. 13. Fiber-to-fiber reflective refractometer (TFBG with a D-shaped fiber) [133].

polarization controlling make the sensor extremely sensitive to slight perturbation over coating layer, such as the bonding of analytes on receptor molecules. The sensor itself is robust, compact in size, ease of use, good stability in physicochemical properties together with remote operation ability, offer them a multitude of opportunities for single-point sensing in hard-to-

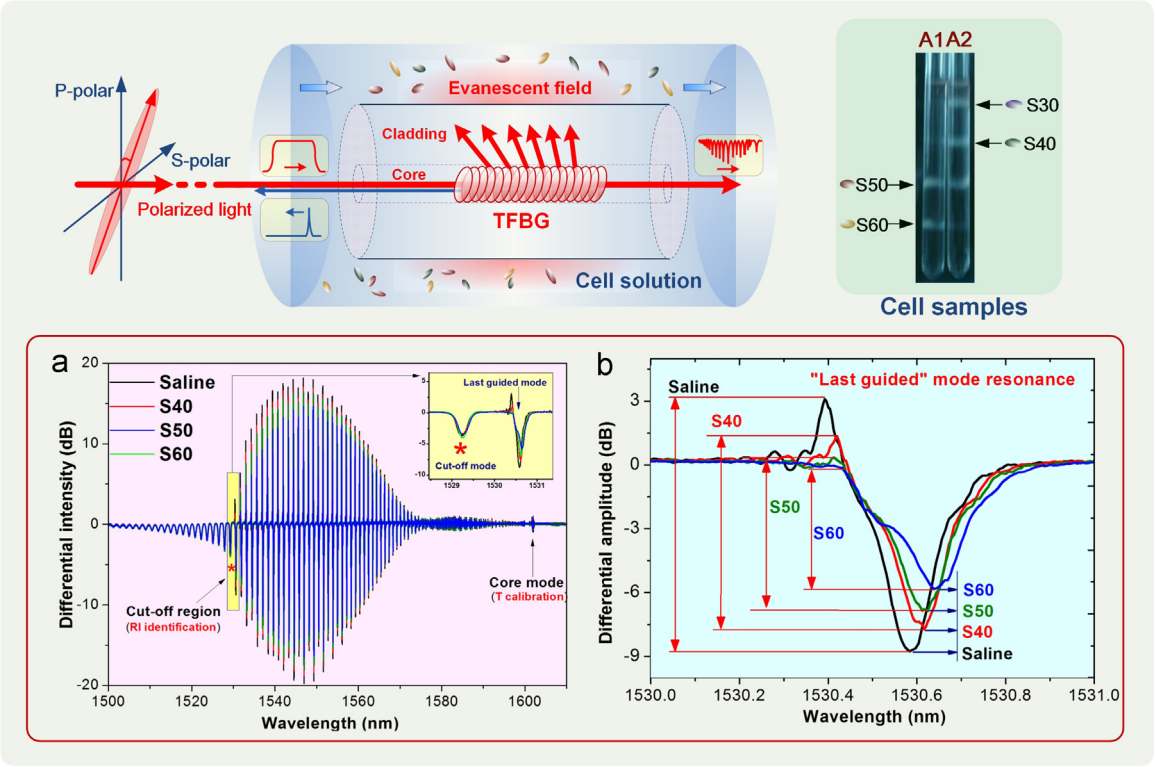

Fig. 14. *In-situ* detection of density alteration in cells (TFBG with two orthogonal polarizations) [75].

reach spaces, even possibly in vivo.

4.2.1. *In-situ detection of density alteration in cells*

By simply using a bare TFBG refractometer, human acute leukemia cells with different intracellular densities and refractive index ranging from 1.3342 to 1.3344 were clearly discriminated *in-situ* [75]. The key point lies in using the differential transmission spectrum between two orthogonal polarizations for the last guided mode resonance before the "cut-off" and leaky mode regime (Fig. 14a), which clearly identifies the most sensitive modal

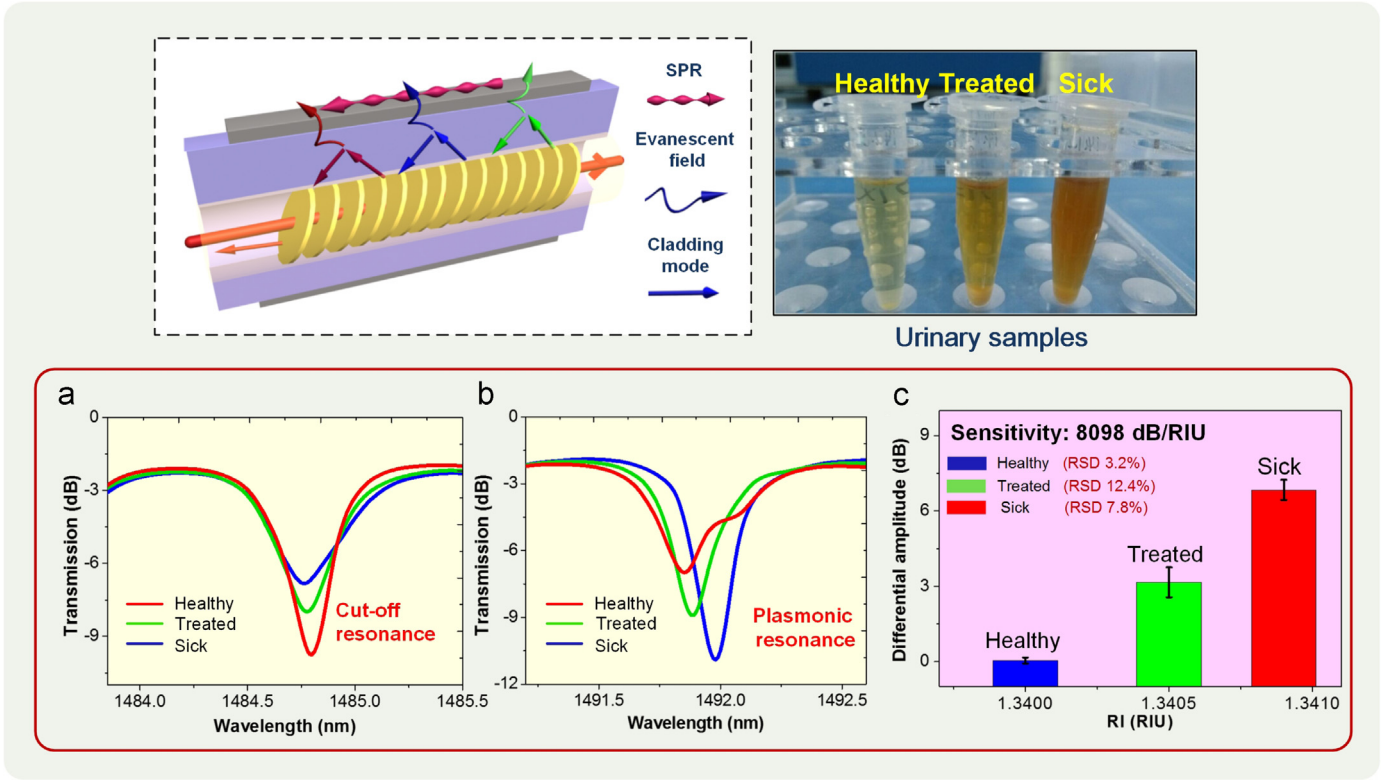

Fig. 15. *In-situ* detection of urinary protein variations (TFBG with ultrathin plasmonic coatings).

resonance. Furthermore the differential spectrum approach automatically cancels the effect of temperature and power level fluctuations. Leukemia cells at various stages of their lives have been discriminated and the associated refractometric sensitivities measured to be 1.8×10^4 dB/RIU, corresponding to a LOD of 2×10^{-5} RIU (Fig. 14b). This study confirms the relationship between the intracellular density of cells and their RI, which might be helpful to the understanding of cell drug resistance of cells, and discovery of new physiological or pathological properties of cells.

4.2.2. In-situ detection of urinary protein variations

The biosensor configuration reported in this work uses a TFBG coated with a nanometer scale silver film. The key point is that by reducing the silver film thickness to around 20–30 nm (rather than 50 nm for optimal SPR excitation), different modes of the TFBG spectrum present very high but opposite sensitivities to RI changes around the TFBG (Fig. 15a and b). Experimental results obtained with the coated TFBG embedded inside a microfluidic channel show an amplitude sensitivity greater than 8000 dB/RIU and a LOD of 10^{-5} RIU (Fig. 15c). Using this device, the effect of different concentrations of protein in rat urine were clearly differentiated between healthy samples, nephropatic samples and samples from individuals under treatment, with a protein concentration sensitivity of 5.5 dB/(mg/ml) and a LOD of 1.5×10^{-3} mg/ml. Those results show a clear relationship between protein outflow and variations in the RI of the urine samples between 1.3400 and 1.3408, pointing the way to the evaluation and development of new drugs for nephropathy treatments. The integration of TFBGs with microfluidic channels enables precise measurement control over samples with sub-microliter volumes and does not require accurate temperature control because of the elimination of the temperature cross-sensitivity inherent in TFBG devices. Integration of the TFBG with a hypodermic needle on the other hand would allow similar measurements in vivo. Work is continuing on this device to further demonstrate the sensor characteristics.

4.2.3. In-situ measurement of glucose concentrations

Different from the traditional plasmonic fiber-optic sensors discussed above, here we takes advantage of the "unsaturated" or "weakened" surface plasmon wave for glucose measurement. The sensing probe used here is a silver-coated plasmonic TFBG. The glucose in human serum is added with a proper GOx. As a consequence, H_2O_2 will be produced due to the effect of enzymatic oxidation. The presence of H_2O_2 will etch the silver coating over the TFBG and therefore remove the SPR attenuation in transmission. The etch rate of the silver coating is proportional to the concentration of the glucose in human serum and this can be unambiguously detected by spectral monitoring of the SPR attenuation in transmission. The simplicity of this homogeneous assay makes it a good candidate for other biochemical detection involving the generation of H_2O_2, such as the detection of choline (catalyzed with choline oxidase), lactic acid (catalyzed with lactate oxidase), glutamate (catalyzed with glutamate oxidase), and organophosphorus neurotoxins (inhibiting the catalytic activity of acetylcholinesterase and choline oxidase), etc. This work is also being pursued to fully charaterize its sensing capabilities (Fig. 16).

5. Conclusions

A review of several of our group's recent and on-going developments in TFBG-based optical fiber sensors has been presented as well as basic theoretical underpinnings of their properties, with reference to other technologies involving fiber cladding modes, i.e. LPGs and "excessively tilted" FBGs. Many of these advances require multidisciplinary teams of engineers, physicists, chemists and biologist because optics cannot "talk" to chemistry and biology without some translation. It is these efforts that are allowing the full potential of such fiber sensors to be reached, and in particular to be able to exploit the extraordinary figures of merit and signal to noise ratio reachable with fiber gratings in simple configurations. It has also been demonstrated that in many of the cases presented, the required instrumentation and protocols are

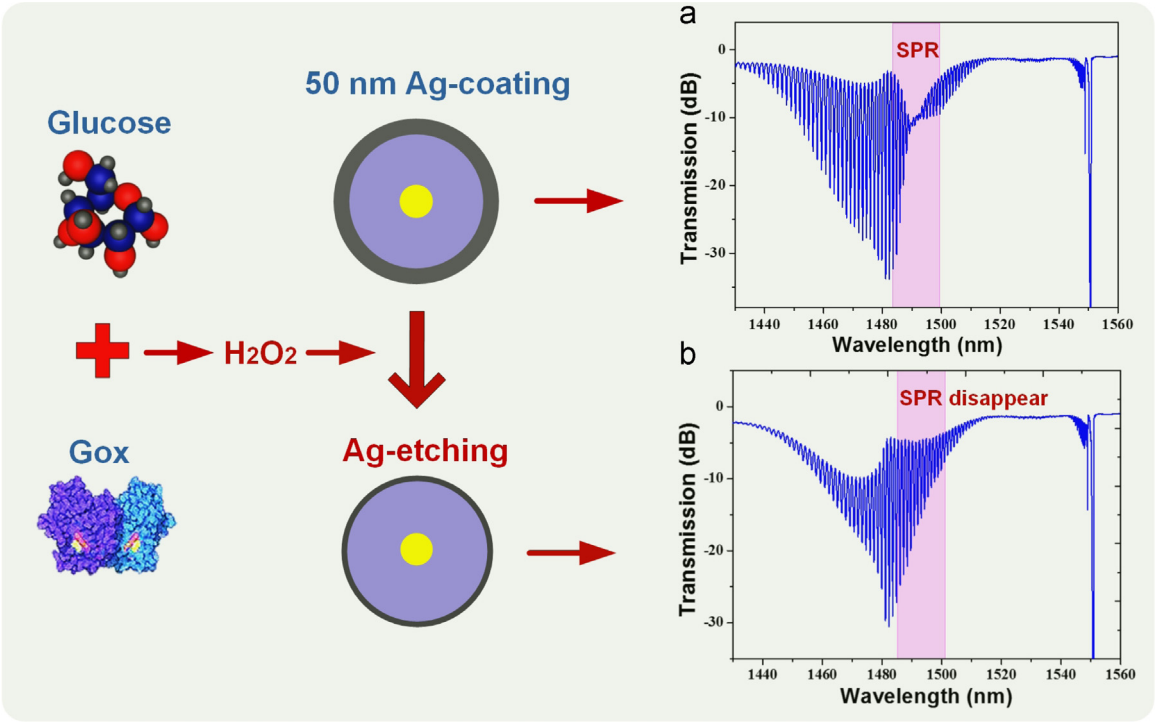

Fig. 16. *In-situ* detection of glucose concentrations (TFBG with etched plasmonic coatings).

sufficiently simple to be implemented in field use or point of care devices at reasonable costs. Where further progress is needed, and this is demonstrated here by two biomedical applications, is in sensing for "real" biofluids, where the materials contain many other substances beyond the desired targets: therefore, in addition to the usual cross-sensitivities (temperature being the most notorious one) "cross-chemical sensitivities" must be addressed, and this can only occur through advanced chemical and biochemical synthesis tools. Among the promising avenues to increased functionalization methods, many nanoscale coatings and structures are currently investigated and will likely lead to progress: microstructured fibers with guiding patterns optimized for sensing [144] (as well as plastic optical fibers [145]) for instance, or the inclusion of other novel functionalized materials (like carbon nanotubes [146], silver nanowires [147], silver nanocubes [148], and graphene [149]), in sensor fabrication. The future is bright indeed for advanced and practical sensing tools using optical fibers.

Acknowledgments

T. Guo and B.O. Guan acknowledge the support of the National Science Fund for Distinguished Young Scholars (No. 61225023), National Natural Science Foundation of China (No. 61205080), the Guangdong Natural Science Foundation of China (No. 2014A030313387), the Youth Science and Technology Innovation Talents of Guangdong (No. 2014TQ01 × 539), the Planned Science and Technology Project of Guangzhou (No. 2012J5100028) and the Fundamental Research Funds for the Central Universities of China (No. 21615446). J. Albert acknowledges the support of the Natural Sciences and Engineering Research Council of Canada (No. RGPIN 2014-05612) and the Canada Research Chairs Program (No. 950-217783).

References

[1] K. Szczerba, P. Westbergh, J. Karout, J. Gustavsson, A. Haglund, M. Karlsson, P. Andrekson, E. Agrell, A. Larsson, 30 Gbps 4-PAM transmission over 200 m of MMF using an 850 nm VCSEL, Opt. Express 19 (2011) B203–B208.
[2] S. Randel, R. Ryf, A. Sierra, P.J. Winzer, A.H. Gnauck, C.A. Bolle, R.J. Essiambre, D.W. Peckham, A. McCurdy, R. Lingle, 6 × 56-Gb/s mode-division multiplexed transmission over 33-km few-mode fiber enabled by 6 × 6 MIMO equalization, Opt. Express 19 (2011) 16697–16707.
[3] J. Wang, J.Y. Yang, I.M. Fazal, N. Ahmed, Y. Yan, H. Huang, Y.X. Ren, Y. Yue, S. Dolinar, M. Tur, A.E. Willner, Terabit free-space data transmission employing orbital angular momentum multiplexing, Nat. Photon. 6 (2012) 488–496.
[4] C. Xia, N. Chand, A.M. Velázquez-Benítez, Z.Q. Yang, X. Liu, J.E. Antonio-Lopez, H. Wen, B.Y. Zhu, N.B. Zhao, F. Effenberger, R. Amezcua-Correa, G.F. Li, Time-division-multiplexed few-mode passive optical network, Opt. Express 23 (2015) 1151–1158.
[5] B. Lee, Review of the present status of optical fiber sensors, Opt. Fiber Technol. 9 (2003) 57–79.
[6] B. Culshaw, Optical fiber sensor technologies: opportunities and-perhaps-pitfalls, J. Lightwave Technol. 22 (2004) 39–50.
[7] K.O. Hill, G. Meltz, Fiber Bragg grating technology fundamentals and overview, J. Lightwave Technol. 15 (1997) 1263–1276.
[8] A.D. Kersey, M.A. Davis, H.J. Patrick, M. LeBlanc, K.P. Koo, C.G. Askins, M. A. Putnam, E.J. Friebele, Fiber grating sensors, J. Lightwave Technol. 15 (1997) 1442–1463.
[9] T. Erdogan, Fiber grating spectra, J. Lightwave Technol. 15 (1997) 1277–1294.
[10] Y.J. Rao, In-fibre Bragg grating sensors, Meas. Sci. Technol. 8 (1997) 355–375.
[11] V. Bhatia, A.M. Vengsarkar, Optical fiber long-period grating sensors, Opt. Lett. 21 (1996) 692–694.
[12] S.W. James, R.P. Tatam, Optical fiber long-period grating sensors: characteristics and application, Meas. Sci. Technol. 14 (2003) R49–R61.
[13] J. Albert, L.Y. Shao, C. Caucheteur, Tilted fiber Bragg grating sensors, Laser Photon. Rev. (2012) 1–26.
[14] Y. Zhao, Q. Wang, H. Huang, Characteristics and applications of tilted fiber Bragg gratings, J. Optoelectron. Adv. Mater. 12 (2010) 2343–2354.
[15] X.Y. Dong, H. Zhang, B. Liu, Y.P. Miao, Tilted fiber Bragg gratings: principle and sensing applications, Photon. Sens. 1 (2011) 6–30.
[16] A.K. Sharma, R. Jha, B.D. Gupta, Fiber-optic sensors based on surface plasmon resonance: a comprehensive review, IEEE Sens. J. 7 (2007) 1118–1129.
[17] J. Albert, S. Lepinay, C. Caucheteur, M.C. DeRosa, High resolution grating-assisted surface plasmon resonance fiber optic aptasensor, Methods 63 (2013) 239–254.
[18] C. Caucheteur, T. Guo, J. Albert, Review of plasmonic fiber optic biochemical sensors: improving the limit of detection, Anal. Bioanal. Chem. 407 (2015) 3883–3897.
[19] M. Li, S.K. Cushing, N.Q. Wu, Plasmon-enhanced optical sensors: a review, Analyst 140 (2015) 386–406.
[20] K.M. Zhou, G. Simpson, X.F. Chen, L. Zhang, I. Bennion, High extinction ratio in-fiber polarizers based on 45° tilted fiber Bragg gratings, Opt. Letters 30 (2005) 1285–1287.
[21] K.M. Zhou, L. Zhang, X.F. Chen, I. Bennion, Low thermal sensitivity grating devices based on Ex-45° tilting structure capable of forward-propagating cladding modes coupling, J. Lightwave Technol. 24 (2006) 5087–5094.
[22] K.M. Zhou, L. Zhang, X.F. Chen, I. Bennion, Optic sensors of high refractive-index responsivity and low thermal cross sensitivity that use fiber Bragg gratings of > 80° tilted structures, Opt. Lett. 31 (2006) 1193–1195.
[23] Z.J. Yan, C.B. Mou, K.M. Zhou, X.F. Chen, L. Zhang, UV-inscription, polarization-dependant loss characteristics and applications of 45° tilted fiber gratings, J. Lightwave Technol. 29 (2011) 2715–2724.
[24] Z.J. Yan, C.B. Mou, H.S. Wang, K.M. Zhou, Y.S. Wang, W. Zhao, L. Zhang, All-fiber polarization interference filters based on 45°-tilted fiber gratings, Opt. Lett. 37 (2012) 353–355.
[25] Z.J. Yan, H.S. Wang, K.M. Zhou, Y.S. Wang, W. Zhao, L. Zhang, Broadband tunable all-fiber polarization interference filter based on 45° tilted fiber gratings, J. Lightwave Technol. 31 (2013) 94–98.
[26] C.B. Mou, K.M. Zhou, L. Zhang, I. Bennion, Characterization of 45°-tilted fiber grating and its polarization function in fiber ring laser, J. Opt. Soc. Am. B 26 (2009) 1905–1911.
[27] X.L. Liu, H.S. Wang, Z.J. Yan, Y.S. Wang, W. Zhao, W. Zhang, L. Zhang, Z. Yang, X.H. Hu, X.H. Li, D.Y. Shen, C. Li, G.D. Chen, All-fiber normal-dispersion single-polarization passively mode-locked laser based on a 45°-tilted fiber grating, Opt. Express 20 (2012) 19000–19005.
[28] Z.J. Yan, H.S. Wang, K.M. Zhou, Y.S. Wang, C. Li, W. Zhao, L. Zhang, Soliton mode locking fiber laser with an all-fiber polarization interference filter, Opt. Lett. 37 (2012) 4522–4524.
[29] X. Chen, K. Zhou, L. Zhang, I. Bennion, In-fiber twist sensor based on a fiber Bragg grating with 81° tilted structure, IEEE Photon. Technol. Lett. 18 (2006) 2596–2598.
[30] C.B. Mou, K.M. Zhou, Z.J. Yan, H.Y. Fu, L. Zhang, Liquid level sensor based on an excessively tilted fibre grating, Opt. Commun. 305 (2013) 271–275.
[31] Z.J. Yan, C.B. Mou, Z.Y. Sun, K.M. Zhou, H.S. Wang, Y.S. Wang, W. Zhao, L. Zhang, Hybrid tilted fiber grating based refractive index and liquid level sensing system, Opt. Commun. 351 (2015) 144–148.
[32] K.S. Feder, P.S. Westbrook, J. Ging, P.I. Reyes, G.E. Carver, In-fiber spectrometer using tilted fiber Gratings, IEEE Photon. Technol. Lett. 15 (2003) 933–935.
[33] C. Jauregui, J.M. Lopez-Higuera, Interrogation of fibre Bragg gratings with a tilted fibre Bragg grating, Meas. Sci. Technol. 15 (2004) 1596–1600.
[34] C. Jáuregui, J.M. López-Higuera, A. Quintela, Interrogation of interferometric sensors with a tilted fiber Bragg grating, Opt. Express 12 (2004) 5646–5654.
[35] S. Wielandy, S.C. Dunn, Tilted superstructure fiber grating used as a Fourier-transform spectrometer, Opt. Lett. 29 (2004) 1614–1616.
[36] C. Yang, Y. Wang, C.Q. Xu, A novel method to measure modal power distribution in multimode fibers using tilted fiber Bragg gratings, IEEE Photon. Technol. Lett. 17 (2005) 2146–2148.
[37] Y. Tissot, H.G. Limberger, R.P. Salathé, Ultrawide bandwidth wavelength monitor based on a pair of tilted fiber Bragg gratings, IEEE Photon. Technol. Lett. 19 (2007) 1702–1704.
[38] R. Suo, X.F. Chen, K.M. Zhou, L. Zhang, I. Bennion, 800 nm WDM interrogation system for strain, temperature, and refractive index sensing based on tilted fiber Bragg grating, IEEE Sens. J. 8 (2008) 1273–1279.
[39] T. Erdogan, J.E. Sipe, Radiation-mode coupling loss in tilted fiber phase gratings, Opt. Lett. 20 (1995) 1838–1840.
[40] T. Erdogan, J.E. Sipe, Tilted fiber phase gratings, J. Opt. Soc. Am. A 13 (1996) 296–313.
[41] T. Erdogan, Cladding-mode resonances in short- and long-period fiber grating filters, J. Opt. Soc. Am. A 14 (1997) 1760–1773.
[42] L. Dong, B. Ortega, L. Reekie, Coupling characteristics of cladding modes in tilted optical fiber Bragg gratings, Appl. Opt. 37 (1998) 5099–5105.
[43] K.S. Lee, T. Erdogan, Fiber mode coupling in transmissive and reflective tilted fiber gratings, Appl. Opt. 39 (2000) 1394–1404.
[44] Y. Koyamada, Analysis of core-mode to radiation-mode coupling in fiber Bragg gratings with finite cladding radius, J. Lightwave Technol. 18 (2000) 1220–1225.
[45] Y.F. Li, M. Froggatt, T. Erdogan, Volume current method for analysis of tilted fiber gratings, J. Lightwave Technol. 19 (2001) 1580–1591.
[46] K.S. Lee, T. Erdogan, Fiber mode conversion with tilted gratings in an optical fiber, J. Opt. Soc. Am. A 18 (2001) 1176–1185.
[47] Y.F. Li, S. Wielandy, G.E. Carver, P.I. Reyes, P.S. Westbrook, Scattering from nonuniform tilted fiber gratings, Opt. Lett. 29 (2004) 1330–1332.
[48] K.S. Lee, T. Erdogan, Transmissive tilted gratings for LP_{01}-to-LP_{11} mode coupling, IEEE Photon. Technol. Lett. 11 (2005) 1286–1288.
[49] Y.F. Li, T.G. Brown, Radiation modes and tilted fiber gratings, J. Opt. Soc. Am. B 23 (2006) 1544–1555.

[50] O. Xu, S.H. Lu, Y. Liu, B. Li, X.W. Dong, L. Pei, S.S. Jian, Analysis of spectral characteristics for reflective tilted fiber gratings of uniform periods, Opt. Commun. 281 (2008) 3990–3995.
[51] S.H. Lu, O. Xu, S.C. Feng, S.S. Jian, Analysis of radiation-mode coupling in reflective and transmissive tilted fiber Bragg gratings, J. Opt. Soc. Am. A 26 (2009) 91–98.
[52] Y.C. Lu, W.P. Huang, S.S. Jian, Full vector complex coupled mode theory for tilted fiber gratings, Opt. Express 18 (2010) 713–726.
[53] J.U. Thomas, N. Jovanovic, R.G. Kramer, G.D. Marshall, M.J. Withford, A. Tunnermann, S. Nolte, M.J. Steel, Cladding mode coupling in highly localized fiber Bragg gratings II: complete vectorial analysis, Opt. Express 20 (2012) 21434–21449.
[54] C.W. Haggans, H. Singh, W.F. Varner, J.S. Wang, Narrow-depressed cladding fiber design for minimization of cladding mode losses in azimuthally asymmetric fiber Bragg gratings, J. Lightwave Technol. 16 (1998) 902–909.
[55] R. Parker, C.M.D. Sterke, Reduced cladding mode losses in tilted gratings that are rotationally symmetric, J. Lightwave Technol. 18 (2000) 2133–2138.
[56] P.S. Westbrook, T.A. Strasser, T. Erdogan, In-line polarimeter using blazed fiber gratings, IEEE Photon. Technol. Lett. 12 (2000) 1352–1354.
[57] S.J. Mihailov, R.B. Walker, P. Lu, H. Ding, X. Dai, C. Smelser, L. Chen, UV-induced polarisation- dependent loss (PDL) in tilted fibre Bragg gratings: application of a PDL equaliser, IEE Proc. Optoelectron. 149 (2002) 211–216.
[58] R.B. Walker, S.J. Mihailov, P. Lu, D. Grobnic, Shaping the radiation field of tilted fiber Bragg gratings, J. Opt. Soc. Am. B 22 (2005) 962–975.
[59] X. Ou, L.S. Hua, J.S. Sheng, Theoretical analysis of polarization properties for tilted fiber Bragg gratings, Sci. China 53 (2010) 390–397.
[60] M.Z. Alam, J. Albert, Selective excitation of radially and azimuthally polarized optical fiber cladding modes, J. Lightwave Technol. 31 (2013) 3167–3175.
[61] K.O. Hill, Y. Fujii, D.C. Johnson, B.S. Kawasaki, Photosensitivity in optical fiber waveguides: application to reflection filter fabrication, Appl. Phys. Lett. 32 (1978) 647–649.
[62] G. Meltz, W.W. Morey, W.H. Glenn, Formation of Bragg gratings in optical fibers by a transverse holographic method, Opt. Lett. 14 (1989) 823–825.
[63] K.O. Hill, B. Malo, F. Bilodeau, D.C. Johnson, J. Albert, Bragg gratings fabricated in monomode photosensitive optical fiber by UV exposure through a phase mask, Appl. Phys. Lett. 62 (1993) 1035–1037.
[64] A. Othonos, Fiber Bragg gratings, Rev. Sci. Instrum. 68 (1997) 4309–4341.
[65] F. Berghmans, T. Geernaert, T. Baghdasaryan, H. Thienpont, Challenges in the fabrication of fibre Bragg gratings in silica and polymer microstructured optical fibres, Laser Photon. Rev. 8 (2014) 27–52.
[66] F. Liu, T. Guo, C. Wu, B.O. Guan, C. Lu, H.Y. Tam, J. Albert, Wideband-adjustable reflection-suppressed rejection filters using chirped and tilted fiber gratings, Opt. Express 22 (2014) 24430–24438.
[67] C. Chen, J. Albert, Strain-optic coefficients of individual cladding modes of singlemode fibre: theory and experiment, Electron. Lett. 42 (2006).
[68] T. Guo, A. Ivanov, C.K. Chen, J. Albert, Temperature-independent tilted fiber grating vibration sensor based on cladding-core recoupling, Opt. Lett. 33 (2008) 1004–1006.
[69] T. Guo, L.Y. Shao, H.Y. Tam, P.A. Krug, J. Albert, Tilted fiber grating accelerometer incorporating an abrupt biconical taper for cladding to core recoupling, Opt. Express 17 (2009) 20651–20660.
[70] G. Laffont, P. Ferdinand, Tilted short-period fibre-Bragg-grating induced coupling to cladding modes for accurate refractometry, Meas. Sci. Technol. 12 (2001) 765–770.
[71] C.F. Chan, C.K. Chen, A. Jafari, A. Laronche, D.J. Thomson, J. Albert, Optical fiber refractometer using narrowband cladding-mode resonance shifts, Appl. Opt. 46 (2007) 1142–1149.
[72] C.Y. Shen, L.Y. Xiong, A. Bialiayeu, Y. Zhang, J. Albert, Polarization-resolved near-and far-field radiation from near-infrared tilted fiber Bragg gratings, J. Lightwave Technol. 32 (2014) 2157–2162.
[73] C.Y. Shen, W.J. Zhou, J. Albert, Polarization-resolved evanescent wave scattering from gold-coated tilted fiber gratings, Opt. Express 22 (2014) 5277–5282.
[74] A. Bialiayeu, A. Ianoul, J. Albert, Polarization-resolved sensing with tilted fiber Bragg gratings: theory and limits of detection, J. Opt. 17 (2015) 1–8.
[75] T. Guo, F. Liu, Y. Liu, N.K. Chen, B.O. Guan, J. Albert, In-situ detection of density alteration in non-physiological cells with polarimetric tilted fiber grating sensors, Biosens. Bioelectron. 55 (2014) 452–458.
[76] P. Berini, Long-range surface plasmon polaritons, Adv. Opt. Photon. 1 (2009) 484–588.
[77] Y. Shevchenko, J. Albert, Plasmon resonances in gold-coated tilted fiber Bragg gratings, Opt. Lett. 32 (2007) 211–213.
[78] T. Allsop, R. Neal, S. Rehman, D.J. Webb, D. Mapps, I. Bennion, Generation of infrared surface plasmon resonances with high refractive index sensitivity utilizing tilted fiber Bragg gratings, Appl. Opt. 46 (2007) 5456–5460.
[79] T. Allop, R. Neal, S. Rehman, D.J. Webb, D. Mapps, I. Bennion, Characterization of infrared surface plasmon resonances generated from a fiber-optical sensor utilizing tilted Bragg gratings, J. Opt. Soc. Am. B 25 (2008) 481–490.
[80] L.Y. Shao, Y. Shevchenko, J. Albert, Intrinsic temperature sensitivity of tilted fiber Bragg grating based surface plasmon resonance sensors, Opt. Express 18 (2010) 11464–11471.
[81] C. Caucheteur, C. Chen, V. Voisin, P. Berini, J. Albert, A thin metal sheath lifts the EH to HE degeneracy in the cladding mode refractometric sensitivity of optical fiber sensors, Appl. Phys. Lett. 99 (2011) 041118.
[82] C.K. Chen, C. Caucheteur, V. Voisin, J. Albert, P. Berini, Long-range surface plasmons on gold-coated single-mode fibers, J. Opt. Soc. Am. B 31 (2014) 2354–2362.
[83] V.M. Cruz, J. Albert, High resolution NIR TFBG-assisted biochemical sensors, J. Lightwave Technol. (2015), http://dx.doi.org/10.1109/JLT.2015.2431912.
[84] S. Baek, Y. Jeong, B. Lee, Characteristics of short-period blazed fiber Bragg gratings for use as macro-bending sensors, Appl. Opt. 41 (2002) 631–636.
[85] B. Liu, Y.P. Miao, H.B. Zhou, Q.D. Zhao, Pure bending characteristic of tilted fiber Bragg grating, J. Electron. Sci. Technol. China 6 (2008) 470–473.
[86] Y.X. Jin, C.C. Chan, X.Y. Dong, Y.F. Zhang, Temperature-independent bending sensor with tilted fiber Bragg grating interacting with multimode fiber, Opt. Commun. 282 (2009) 3905–3907.
[87] L.Y. Shao, A. Laronche, M. Smietana, P. Mikulic, W.J. Bock, J. Albert, Highly sensitive bend sensor with hybrid long-period and tilted fiber Bragg grating, Opt. Commun. 283 (2010) 2690–2694.
[88] L.Y. Shao, L.Y. Xiong, C.K. Chen, A. Laronche, J. Albert, Directional bend sensor based on re-grown tilted fiber Bragg grating, J. Lightwave Technol. 28 (2010) 2681–2687.
[89] L.Y. Shao, J. Albert, Compact fiber-optic vector inclinometer, Opt. Lett. 35 (2010) 1034–1036.
[90] C.X. Guo, D.B. Chen, C.Y. Shen, Y.F. Lu, H.N. Liu, Optical inclinometer based on a tilted fiber Bragg grating with a fused Taper, Opt. Fiber Technol. 24 (2015) 30–33.
[91] L.Y. Shao, Q. Jiang, J. Albert, Fiber optic pressure sensing with conforming elastomers, Appl. Opt. 49 (2010) 6784–6788.
[92] L.Y. Shao, J. Albert, Lateral force sensor based on a core-offset tilted fiber Bragg grating, Opt. Commun. 284 (2011) 1855–1858.
[93] T. Guo, C.K. Chen, J. Albert, Non-uniform-tilt-modulated fiber Bragg grating for temperature-immune micro-displacement measurement, Meas. Sci. Technol. 20 (2009) 034007.
[94] P. Ivanoff, D.C. Reyes, P.S. Westbrook, P.D.L. Tunable, of twisted–tilted fiber gratings, IEEE Photon. Technol. Lett. 15 (2003) 828–830.
[95] T. Guo, F. Liu, B.O. Guan, J. Albert, Polarimetric multi-mode tilted fiber grating sensors, Opt. Express 22 (2014) 7330–7336.
[96] C. Shen, Y. Zhang, W.J. Zhou, J. Albert, Au-coated tilted fiber Bragg grating twist sensor based on surface plasmon resonance, Appl. Phys. Lett. 104 (2014) 071106.
[97] Y.F. Lu, C.Y. Shen, D.B. Chen, J.L. Chu, Q. Wang, X.Y. Dong, Highly sensitive twist sensor based on tilted fiber Bragg grating of polarization-dependent properties, Opt. Fiber Technol. 20 (2014) 491–494.
[98] M.Y. Fu, W.F. Liu, T.C. Chen, Effect of acoustic flexural waves in a tilted superstructure fiber grating, Opt. Eng. 44 (2005) 024401.
[99] Y.H. Huang, T. Guo, C. Lu, H.Y. Tam, VCSEL-based tilted fiber grating vibration sensing system, IEEE Photon. Technol. Lett. 22 (2010) 1235–1357.
[100] T. Guo, L.B. Shang, Y. Ran, B.O. Guan, J. Albert, Fiber-optic vector vibroscope, Opt. Lett. 37 (2012) 2703–2705.
[101] M. Li, L.Y. Shao, J. Albert, J.P. Yao, Continuously tunable photonic fractional temporal differentiator based on a tilted fiber Bragg grating, IEEE Photon. Technol. Lett. 23 (2011) 251–253.
[102] M. Li, L.Y. Shao, J. Albert, J.P. Yao, Tilted fiber Bragg grating for chirped microwave waveform generation, IEEE Photon. Technol. Lett. 23 (2011) 314–316.
[103] S.C. Kang, S.Y. Kim, S.B. Lee, S.W. Kwon, S.S. Choi, B. Lee, Temperature-independent strain sensor system using a tilted fiber Bragg grating dmodulator, IEEE Photon. Technol. Lett. 10 (1998) 1461–1463.
[104] Z.Y. Zhao, S. Zhang, Y.S. Yu, Z.C. Zhuo, J. Zhang, W. Zheng, Y.S. Zhang, Fabrication of a tilted fiber Bragg grating with a designed reflection spectrum profile, Opt. Lett. 29 (2004) 244–246.
[105] Y.P. Miao, B. Liu, W.H. Zhang, B. Dong, H.B. Zhou, Q.D. Zhao, Dynamic temperature compensating interrogation technique for strain sensors with tlted fiber Bragg gratings, IEEE Photon. Technol. Lett. 20 (2008) 1393–1395.
[106] M. Pisco, A. Ricciardi, S. Campopiano, C. Caucheteur, P. Megret, A. Cusano, Time delay measurements as promising technique for tilted fiber Bragg grating sensors interrogation, IEEE Photon. Technol. Lett. 21 (2009) 1752–1754.
[107] B. Zhou, A.P. Zhang, S. He, B.B. Gu, Cladding-mode-recoupling-based tilted fiber Bragg grating sensor with a core-diameter-mismatched fiber section, IEEE Photon. Sens. J. 2 (2010) 152–157.
[108] F. Baldini, M. Brenci, F. Chiavaioli, A. Giannetti, C. Trono, Optical fibre gratings as tools for chemical and biochemical sensing, Anal. Bioanal. Chem. 402 (2012) 109–116.
[109] X.D. Wang, O.S. Wolfbeis, Fiber-optic chemical sensors and biosensors (2008–2012), Anal. Chem. 85 (2013) 487–508.
[110] X.D. Fan, I.M. White, S.I. Shopova, H.Y. Zhu, J.D. Suter, Y.Z. Sun, Sensitive optical biosensors for unlabeled targets: a review, Anal. Chim. Acta 620 (2008) 8–26.
[111] D. Paladino, G. Quero, C. Caucheteur, P. Megret, A. Cusano, Hybrid fiber grating cavity for multi-parametric sensing, Opt. Express 18 (2010) 10473–10486.
[112] A.C.L. Wong, W.H. Chung, C. Lu, H.Y. Tam, Composite structure distributed Bragg reflector fiber laser for simultaneous two-parameter sensing, IEEE Photon. Technol. Lett. 22 (2010) 1464–1466.
[113] A.C.L. Wong, M. Giovinazzo, H.Y. Tam, C. Lu, G.D. Peng, Simultaneous two-parameter sensing using a single tilted moiré fiber Bragg grating with discrete wavelet transform technique, IEEE Photon. Technol. Lett. 22 (2010) 1574–1576.
[114] A.C.L. Wong, W.H. Chung, H.Y. Tam, C. Lu, Single tilted Bragg reflector fiber laser for simultaneous sensing of refractive index and temperature, Opt. Express 19 (2011) 409–414.

[115] X.F. Chen, K.M. Zhou, L. Zhang, I. Bennion, Optical chemsensor based on etched tilted Bragg grating structures in multimode fiber, IEEE Photon. Technol. Lett. 17 (2005) 864–865.
[116] C. Caucheteur, D. Paladino, P. Pilla, A. Cutolo, S. Campopiano, M. Giordano, A. Cusano, P. Megret, External refractive index sensitivity of weakly tilted fiber Bragg gratings with different coating thicknesses, IEEE Sens. J. 8 (2008) 1330–1336.
[117] D.J. Mandia, M.B.E. Griffiths, W.J. Zhou, P.G. Gordon, J. Albert, S.T. Barry, In situ deposition monitoring by a tilted fiber Bragg grating optical probe: probing nucleation in chemical vapour deposition of gold, Phys. Proc. 46 (2013) 12–20.
[118] J.M. Renoirt, C. Zhang, M. Debliquy, M.G. Olivier, P. Megret, C. Caucheteur, High-refractive-index transparent coatings enhance the optical fiber cladding modes refractometric sensitivity, Opt. Express 21 (2013) 29073–29082.
[119] S. Lepinay, A. Ianoul, J. Albert, Molecular imprinted polymer-coated optical fiber sensor for the identification of low molecular weight molecules, Talanta 128 (2014) 401–407.
[120] W.J. Zhou, D.J. Mandia, S.T. Barry, J. Albert, Anisotropic effective permittivity of an ultrathin gold coating on optical fiber in air, water and saline solutions, Opt. Express 22 (2014) 31665–31676.
[121] Y.P. Miao, B. Liu, H. Zhang, Y. Li, H.B. Zhou, H. Sun, W.H. Zhang, Q.D. Zhao, Relative humidity sensor based on tilted fiber Bragg grating with polyvinyl alcohol coating, IEEE Photon. Technol. Lett. 21 (2009) 441–443.
[122] J.Y. Yang, X.Y. Dong, K. Ni, C.C. Chan, P.P. Shun, Intensity-modulated relative humidity sensing with polyvinyl alcohol coating and optical fiber gratings, Appl. Opt. 54 (2015) 2620–2624.
[123] S. Lepinay, A. Ianoul, J. Albert, Tilted fiber Bragg gratings as a new sensing device for in situ and real time monitoring of surface initiated polymerization, Talanta 128 (2014) 401–407.
[124] C. Caucheteur, M. Wuilpart, C.K. Chen, P. Megret, J. Albert, Quasi-distributed refractometer using tilted Bragg gratings and time domain reflectometry, Opt. Express 16 (2008) 17882–17890.
[125] C. Caucheteur, P. Megret, A. Cusano, Tilted Bragg grating multipoint sensor based on wavelength-gated cladding-modes coupling, Appl. Opt. 48 (2009) 3915–3920.
[126] Y.Q. Liu, Q. Liu, K.S. Chiang, Optical coupling between a long-period fiber grating and a parallel tilted fiber Bragg grating, Opt. Lett. 34 (2009) 1726–1728.
[127] T. Guo, H.Y. Tam, P.A. Krug, J. Albert, Reflective tilted fiber Bragg grating refractometer based on strong cladding to core recoupling, Opt. Express 17 (2009) 5736–5742.
[128] B.B. Gu, W.L. Qi, J. Zheng, Y.Y. Zhou, P.P. Shum, F. Luan, Simple and compact reflective refractometer based on tilted fiber Bragg grating inscribed in thin-core fiber, Opt. Lett. 39 (2014) 22–25.
[129] T. Guo, C.K. Chen, A. Laronche, J. Albert, Power-referenced and temperature-calibrated optical fiber refractometer, IEEE Photon. Technol. Lett. 20 (2008) 635–637.
[130] Y.P. Miao, B. Liu, Q.D. Zhao, Refractive index sensor based on measuring the transmission power of tilted fiber Bragg grating, Opt. Fiber Technol. 15 (2009) 233–236.
[131] T. Li, X.Y. Dong, C.C. Chan, C.L. Zhao, S.Z. Jin, Power-referenced optical fiber refractometer based on a hybrid fiber grating, IEEE Photon. Technol. Lett. 23 (2011) 1706–1708.
[132] J. Zheng, X.Y. Dong, J.H. Ji, H.B. Su, P.P. Shum, Power-referenced refractometer with tilted fiber Bragg grating cascaded by chirped grating, Opt. Commun. 312 (2014) 106–109.
[133] Z.Y. Cai, F. Liu, T. Guo, B.O. Guan, G.D. Peng, J. Albert, Evanescently coupled optical fiber refractometer based a tilted fiber Bragg grating and a D-shaped fiber, Opt. Express 23 (2015) 20971–20976.
[134] Y. Shevchenko, T.J. Francis, D.A.D. Blair, R. Walsh, M.C. Derosa, J. Albert, In situ biosensing with a surface plasmon resonance fiber grating aptasensor, Anal. Chem. 83 (2011) 7027–7034.
[135] A. Bialiayeu, C. Caucheteur, N. Ahamad, A. Ianoul, J. Albert, Self-optimized metal coatings for fiber plasmonics by electroless deposition, Opt. Express 19 (2011) 18742–18753.
[136] L.Y. Shao, J.P. Coyle, S.T. Barry, J. Albert, Anomalous permittivity and plasmon resonances of copper nanoparticle conformal coatings on optical fibers, Opt. Mater. Express 1 (2011) 128–137.
[137] V. Voisin, J. Pilate, P. Damman, P. Megret, C. Caucheteur, Highly sensitive detection of molecular interactions with plasmonic optical fiber grating sensors, Biosens. Bioelectron. 51 (2014) 249–254.
[138] Y. Shevchenko, G.C. Unal, D.F. Cuttica, M.R. Dokmeci, J. Albert, A. Khademhosseini, Surface plasmon resonance fiber sensor for real-time and label-free monitoring of cellular behavior, Biosens. Bioelectron. 56 (2014) 359–367.
[139] K. Chah, V. Voisin, D. Kinet, C. Caucheteur, Surface plasmon resonance in eccentric femtosecond laser- induced fiber Bragg gratings, Opt. Lett. 39 (2014) 6887–6890.
[140] C. Caucheteur, V. Voisin, J. Albert, Near-infrared grating-assisted SPR optical fiber sensors: design rules for ultimate refractometric sensitivity, Opt. Express 23 (2015) 2918–2932.
[141] V. Malachovska, C. Ribaut, V. Voisin, M. Surin, P. Leclere, R. Wattiez, C. Caucheteur, Fiber-optic SPR immunosensors tailored to target epithelial cells through membrane receptors, Anal. Chem. (2015), http://dx.doi.org/10.1021/acs.analchem.5b00159.
[142] M.D. Baiad, R. Kashyap, Concatenation of surface plasmon resonance sensors in a single optical fiber using tilted fiber Bragg gratings, Opt. Lett. 40 (2015) 115–117.
[143] X.H. Hu, P. Megret, C. Caucheteur, Surface plasmon excitation at near-infrared wavelengths in polymer optical fibers, Opt. Lett. 40 (2015) 3998–4001.
[144] M.C.P. Huy, G. Laffout, V. Dewynter, P. Ferdinand, Tilted fiber Bragg grating photowritten in microstructured optical fiber for improved refractive index measurement, Opt. Express 14 (2006) 10359–10370.
[145] X.H. Hu, C.F.J. Pun, H.Y. Tam, P. Mégret, C. Caucheteur, Tilted Bragg gratings in step-index polymer optical fiber, Opt. Lett. 39 (2014) 6835–6838.
[146] G.E. Villanueva, M.B. Jakubinek, B. Simard, C.J. Oton, Linear and nonlinear optical properties of carbon nanotube-coated single-mode optical fiber gratings, Opt. Lett. 36 (2011) 2104–2106.
[147] J.M. Renoirt, M. Debliquy, J. Albert, A. Ianoul, C. Caucheteur, Surface plasmon resonances in oriented silver nanowire coatings on optical fibers, J. Phys. Chem. 118 (2014) 11035–11042.
[148] A. Lanoul, M. Robson, V. Pripotnev, J. Albert, Polarization-selective excitation of plasmonic resonances in silver nanocube random arrays by optical fiber cladding mode evanescent fields, RSC Adv., 4, (2014) 19725–19730.
[149] B.Q. Jiang, X. Lu, X.T. Gan, M. Qi, Y.D. Wang, L. Han, D. Mao, W.D. Zhang, Z. Y. Ren, J.L. Zhao, Graphene-coated tilted fiber-Bragg grating for enhanced sensing in low-refractive-index region, Opt. Lett. 40 (2015) 3994–3996.